CERN-INTC-2016-031 / INTC-P-398-ADD-1
01/06/2016

EUROPEAN ORGANIZATION FOR NUCLEAR RESEARCH

Addendum to the ISOLDE and Neutron Time-of-Flight Committee

IS587: Characterising excited states in and around the semi-magic nucleus ^{68}Ni using Coulomb excitation and one-neutron transfer

June 1, 2016

L. P. Gaffney[1], P. Van Duppen[2], F. Flavigny[3], M. Zielińska[4], K. Kolos[5], A. N. Andreyev[6], M. Axiotis[7], D. L. Balabanski[8], A. Blazhev[9], J. Cederkäll[10], T. E. Cocolios[11], E. Clément[12], T. Davinson[13], G. De France[12], H. De Witte[2], D. Di Julio[10], T. Duguet[4], C. Fahlander[10], S. J. Freeman[11], G. Georgiev[14], R. Gernhäuser[15], A. Gillibert[4], S. Go[16], T. Grahn[17], P. T. Greenlees[17], R. K. Grzywacz[16,18], S. Harissopulos[7], M. Huyse[2], A. Illana[2], D. G. Jenkins[6], J. Jolie[9], R. Julin[17], M. Komorowska[4,19], W. Korten[4], Th. Kröll[20], A. Lagoyannis[7], C. Louchart[4], T. Marchi[2], T. J. Mertzimekis[21], D. Miller[21], D. Mücher[22,23], P. Napiorkowski[19], K. Nowak[15], F. Nowacki[24], D. O'Donnell[1], A. Obertelli[4], R. Orlandi[24], T. Otsuka[26], J. Pakarinen[17], P. Papadakis[17], N. Patronis[27], N. Pietralla[20], P. Rahkila[17], R. Raabe[2], G. Rainovski[28], E. Rapisarda[29], P. Reiter[9], M. Scheck[1], M. Seidlitz[9], B. Siebeck[9], K. Sieja[24], D. K. Sharp[11], J. F. Smith[1], C. Sotty[2], O. Sorlin[12], J. Srebrny[19], M. J. Taylor[11], Y. Tsunoda[26], N. Warr[9], R. Wadsworth[6], F. Wenander[29], K. Wimmer[26], P. J. Woods[13], K. Wrzosek-Lipska[19]

[1] *University of the West of Scotland, U.K.* | [2] *KU Leuven, Belgium* | [3] *IPN Orsay, France* | [4] *CEA-Saclay, France* | [5] *Lawrence Livermore National Laboratory, U.S.A.* | [6] *University of York, U.K.* | [7] *NCSR-Demokritos, Greece* | [8] *INRNE-BAS, Bulgaria* | [9] *University of Köln, Germany* | [10] *University of Lund, Sweden* | [11] *University of Manchester, U.K.* | [12] *GANIL, France* | [13] *University of Edinburgh, U.K.* | [14] *CSNSM, France* | [15] *TU-München, Germany* | [16] *University of Jyväskylä and Helsinki Institute of Physics, Finland* | [17] *University of Tennessee, Knoxville, U.S.A.* | [18] *Oak Ridge National Laboratory, U.S.A.* | [19] *HIL, University of Warsaw, Poland* | [20] *TU-Darmstadt, Germany* | [21] *University of Athens, Greece* | [22] *TRIUMF, Canada* | [23] *University of Guelph, Canada* | [24] *Université de Strasbourg, France* | [25] *JAEA, Tokai, Japan* | [26] *University of Tokyo, Japan* | [27] *University Of Ioannina, Greece* | [28] *St. Kl. Ohridski University of Sofia, Bulgaria* | [29] *CERN-ISOLDE, Switzerland*

Spokespersons: L. P. Gaffney [Liam.Gaffney@uws.ac.uk], P. Van Duppen [Piet.VanDuppen@fys.kuleuven.be], F. Flavigny [flavigny@ipno.in2p3.fr], M. Zielińska [magda.zielinska@cea.fr], K. Kolos [kolos1@llnl.gov]
Contact person: K. Johnston [Karl.Johnston@cern.ch]

Abstract: It is proposed to investigate the structure of excited states in ^{66,68,70}Ni($Z = 28, N = 38, 40, 42$) via the measurement of electromagnetic matrix elements in a Coulomb-excitation experiment. The aim is to study the $N = 40$ sub-shell and the $Z = 28$ proton shell closures, where predictions of shape coexistence and islands of inversion remain unsatisfactorily tested. The crucial observables in this study will be the spectroscopic quadrupole moments of the 2_1^+ state, Q_s, and the $B(E2; 2_1^+ \rightarrow 0_1^+)$. Both of these quantities in combination reveal substantial

information about the structure and collective shape of the states, while also testing the predictive power of different nuclear models. Low-energy Coulomb excitation is the only method sensitive to $Q_s(2^+)$ and HIE-ISOLDE is the only facility world-wide presently capable of such an experiment. In addition, new Monte-Carlo Shell-Model (MCSM) calculations predict shape coexistence in ^{68}Ni and neighbouring isotopes. By measuring electromagnetic matrix elements connecting excited states, a direct comparison to theory can be made. Utilising the increased energy provided by the HIE-ISOLDE upgrade, multi-step Coulomb excitation will give sensitivity to $E2$ matrix elements connecting the 2_1^+ state with 0_2^+ and potentially 2_2^+ states. This addendum follows on from proposal P398 [1], for which nine shifts were granted for the transfer part of the experiment (IS587), but as yet none for the Coulomb-excitation part.

Requested shifts: 33 shifts (in addition to the 9 shifts already granted)

1 Introduction and physics case

The physics case for this work has been laid out in the original proposal [1]. The strong theoretical [2, 3] and experimental [4–10] interest in the ^{68}Ni region has only heightened in the meantime. Recently, large-scale shell-model calculations have described the appearance of shape coexistence in ^{78}Ni and a new island of inversion about ^{74}Cr [11], similar to that proposed about ^{64}Cr [12]. This comes on the back of high-profile experimental efforts in this extremely exotic region [13–15]. However, if we are to reach forward both theoretically and experimentally to the most exotic systems approaching ^{78}Ni, we must make detailed and precision measurements testing the latest shell-model calculations to the fullest. The more experimentally attainable region about ^{64}Cr/^{68}Ni, with strong similarities to newly proposed island of inversion about ^{74}Cr/^{78}Ni [11, 12], can be used as a benchmark particularly with the potential to measure electromagnetic properties to high precision.

Each of the previous Coulex experiments studying ^{66,68,70}Ni were performed at relativistic energies, with the exception of the low-statistics measurement of ^{68}Ni at REX-ISOLDE [16]. Aside from the low precision, the conditions of the former type of measurement, such as unobserved feeding from higher-energy 2^+ states, could systematically affect the determination of the transition strengths. This would lead to inaccurate results and a measurement free of any experimental bias, is required to reconcile the situation before further theoretical interpretations can be made. Low-energy Coulomb excitation is the only technique sensitive to the spectroscopic quadrupole moments of the excited states and measuring $Q_s(2_1^+)$ in ^{68}Ni will settle the long-standing discussion over the nature of this state. Opening the possibility to multi-step Coulomb excitation in these nuclei, the higher energy provided by the HIE-ISOLDE upgrade will allow for determination of $E2$ matrix elements connecting the 2_1^+ state with 0_2^+ and potentially 2_2^+ states.

Recent state-of-the-art Monte-Carlo shell-model (MCSM) calculations [2] have proposed the existence of shape coexistence in ^{68}Ni, termed *Type II shell evolution*. In particular, the results of the calculations conclude that the first-excited 2^+ state belongs to an oblate-deformed intruder structure, something that can be tested directly via a measurement of the spectroscopic quadrupole moment, Q_s. The rigid-rotor model of Bohr and Mottelson gives a relationship for matrix elements between excited nuclear states with the same intrinsic quadrupole moment, Q_0, as follows.

$$\langle I_f||E\lambda||I_i\rangle = \sqrt{\frac{5(2I_f+1)}{16\pi}}\langle I_f 020|I_i 0\rangle Q_0. \quad (1)$$

Assuming the 0_1^+ ground-state and the first-excited 2_1^+ state in ^{68}Ni are of the same structure,

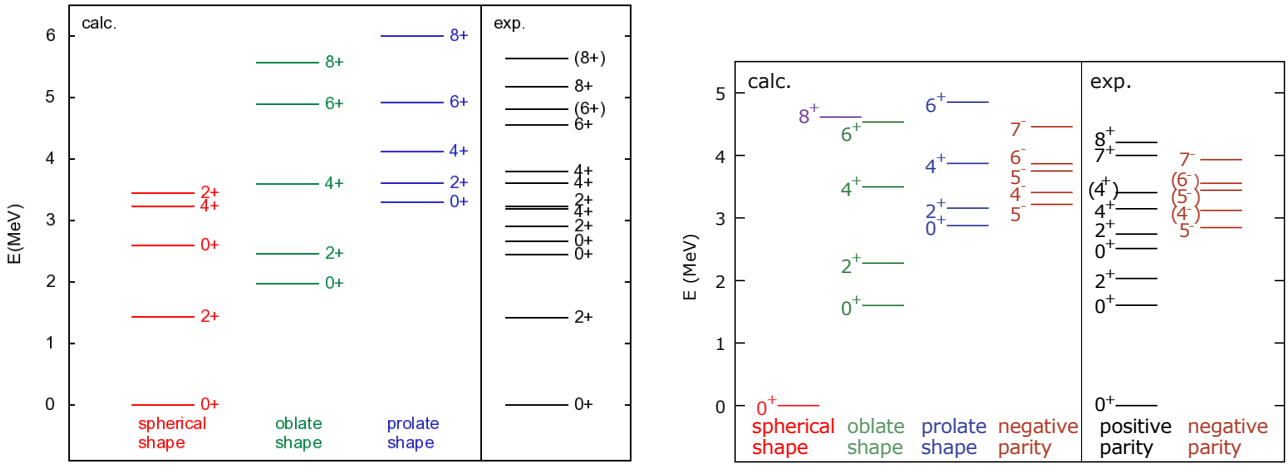

Figure 1: Level schemes of ^{66}Ni (left) and ^{68}Ni (right) obtained from the Monte-Carlo shell model calculations [2] compared to the experimentally observed levels.

the ratio of the transitional and diagonal $E2$ matrix elements would reduce to a ratio of spin factors and Clebsch-Gordan coefficients, which can be stated as,

$$\left|\frac{\langle 2_1||E2||2_1\rangle}{\langle 0_1||E2||2_1\rangle}\right| = 1.195. \tag{2}$$

Using the previously measured $B(E2; 2_1^+ \rightarrow 0_1^+)$ in ^{68}Ni and Equation 2, we expect that $|Q_s| = 14.7\ e\text{fm}^2$. The MCSM calculations [2] predict that the 2_1^+ state is oblate with $Q_s \simeq 27\ e\text{fm}^2$, being associated to the 0_2^+ state, while the spherical 2^+ state lies at much higher energy. If this is correct, then the measured value Q_s would be inconsistent with the naïve rigid-rotor model assumption, an unambiguous way of proving that the 2_1^+ state belongs to an intruder structure with oblate deformation. The γ-ray branching ratio with respect to the $0_{1,2}^+$ states would in turn lead to an understanding of the structure of $0_{1,2}^+$ states. Unfortunately, in a recent β-decay at the Isolde Decay Station (IDS), it was not possible to observe this branching ratio [17], however, multi-step Coulomb excitation is sensitive to the absolute $B(E2; 2_1^+ \rightarrow 0_2^+)$ value via the experimentally observed 0_2^+ population, as detailed in the original proposal [1]. The energies of the calculated and experimentally observed states are shown on the right-hand side of Fig. 1.

In ^{70}Ni, it is predicted that the supposed oblate configuration becomes the ground state with its associated 2^+ state being the first-excited state [2]. Further, it is expected that a 0_2^+ state exists in this nucleus, which is prolate in character and associated with a 2^+ state measured at 1.867 MeV. This could describe the newly discovered state at 1.567 MeV by Prokop et. al [8]. The technique of Coulomb excitation is well suited to populating low-spin non-yrast states and a verification of the new 0_2^+ state would be possible via a two-step excitation. Furthermore, a discrepancy of a factor of four exists in the $B(E2; 2_1^+ \rightarrow 0_1^+)$ values of ^{70}Ni between those measured via intermediate-energy Coulex [18] and direct lifetime measurements [19]. Newly measured $B(E2)$ values in the heavier isotopes of ^{72}Ni [10] and ^{74}Ni [7] contradict the established trend, supported by shell-model calculations with both the LNPS interaction [12] and the MCSM approach [2]. A lower than expected $B(E2; 2_1^+ \rightarrow 0_1^+)$ value would contradict the interpretation of proton-core polarisation in ^{70}Ni due to occupancy of the $\nu g_{9/2}$ orbital [18]. A precise measurement of this value is required to resolve the current discrepancies with theory and experiment.

Below $N = 40$ in ^{66}Ni, a vibrational-like structure is predicted for the ground state and first-excited 2^+ state, yielding $Q_s(2^+) = 19\ e\text{fm}^2$ [2]. The oblate intruder structure has a predicted

band-head energy of about 2.0 MeV. Furthermore, a prolate structure appears in calculations above 3.0 MeV, similar to the configuration proposed for the 0_3^+ state in ^{68}Ni and 0_2^+ state in ^{70}Ni, strongly favouring the description of shape coexistence. By measuring the electromagnetic matrix elements of ^{66}Ni in the same campaign we will not only provide further information on intruder configurations about $N = 40$, but also have a higher statistics data set to verify our treatment of uncertainties in ^{68,70}Ni. The large production yield also leads to a significant population of states via two-step Coulomb excitations, crucially the 0_2^+, enabling a measurement of the $E2$ matrix element, $\langle 2_1^+ \| E2 \| 0_2^+ \rangle$. This value, in combination with $B(E2; 2_1^+ \rightarrow 0_1^+)$ and $Q_s(2^+)$, is an extremely sensitive probe of the structure of the 2_1^+ and 0_2^+ states and can be directly compared to the MCSM calculations [2] that predict shape coexistence.

We propose to perform Coulomb excitation of the ^{66,68}Ni projectiles from HIE-ISOLDE at an energy of 4.0 MeV/u and of ^{70}Ni at 3.5 MeV/u. The secondary target employed will be ^{206}Pb in order to provide a normalisation to the target excitation. The aim is to determine the $B(E2)$ values in ^{66,68,70}Ni connecting ground and excited 0^+ and 2^+ states and, simultaneously, $Q_s(2_1^+)$ in these nuclei.

2 Experimental Method

Method – Coulomb excitation (Coulex) at "safe" energies is an excellent tool to measure transition strengths connecting low-lying states. "Safe" Coulex implies that the bombarding energy is far enough below the Coulomb barrier that the interacting nuclear surfaces are separated by a minimum distance of 5 fm, keeping the interaction purely electromagnetic. Intermediate-energy or relativistic Coulomb excitation is usually restricted to single-step excitations. Measuring as close to the Coulomb barrier as possible in "safe" Coulex however, and for a wide range of scattering angles, will lead to higher-order excitations. Crucially, one such higher-order process is the reorientation effect [20] meaning that the excitation cross sections are sensitive to the spectroscopic quadrupole moments.

Beam energy – To ensure the safe condition is met, a balance has to be struck between beam energy and the maximum centre-of-mass (CoM) scattering angle. In order to enhance the crucial second-order excitations, the highest CoM angles are desired and therefore lower beam energies are needed. An optimisation of the beam energy has been performed using the GOSIA code to obtain the best sensitivity for $Q_s(2_1^+)$ and it is found to be at 4.0 MeV/u. The limit in CoM scattering angle is indicated on Figure 2. For ^{70}Ni, where sensitivity to $Q_s(2_1^+)$ is not required, it is preferable to maintain the safe energy criterion for all scattering angles of the detected projectiles and recoils, meaning a maximum beam energy of 3.5 MeV/u.

Setup – The Miniball Ge-detector array [21] will be used to detect the de-excitation γ rays following Coulomb excitation. The T-REX Si-detector array [22] allows for particle detection and identification at forward laboratory angles by utilising a Double-Sided Silicon Strip Detector (DSSSD), or CD detector, plus four barrel detectors. In the backward laboratory angles, the same system of four barrel detectors plus CD detector is repeated. We do not intend to use the barrel detectors in the forward direction to allow the CD detector to be brought into a close geometry at 28 mm from the target, where the angular coverage is 17.9°–55.6° in the laboratory. The backward angles will be configured for the transfer part of the original proposal [1]. It would also be possible to use the standard Coulex setup consisting of only the CD detector at forward angles, this allowing the flexibility to schedule the two parts of the proposal independently. Angle-dependent software gates on particle energy can be used to identify projectiles and recoils and make cuts corresponding to the appropriate centre-of-mass

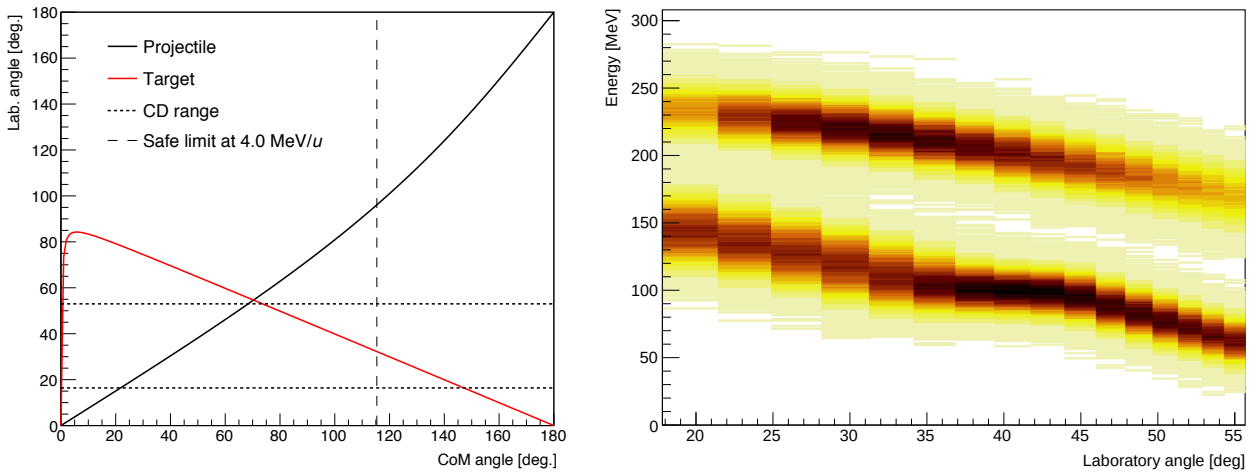

Figure 2: Simulated kinematics for a two-body reaction of a ^{68}Ni projectile (red line on left panel; lower-most kinematic curve on the right panel) at 4.0 MeV/u incident on a ^{206}Pb target (black line; upper-most curve) of thickness 2.0 mg/cm^2. On the left panel, the laboratory angles of the scattered projectiles and target particles correspond to unique centre-of-mass scattering angle solutions, allowing maximum coverage of the centre-of-mass angular range. On the right panel separation of the scattering partners in energy and angle is evidenced.

solutions. Simulations of the kinematics have been made, as shown in Figure 2 where it can be observed that the projectile and recoil can be cleanly separated. The granularity of the MINIBALL array and the CD detector allows for Doppler correction to be applied to γ rays emitted in flight.

3 Beam-time Request

^{68}***Ni*** – We estimate a beam intensity at Miniball of 1.0×10^5 ions/s; assuming a proton current of 2 μA and a primary yield of 1.0×10^6 ions/μC. We have revised the post-acceleration efficiency estimate to 5%. In order to estimate the expected γ-ray intensities, the computer code GOSIA has been employed [23, 24]. The Coulomb-excitation cross section for each state is calculated for a large number of angle and energy meshpoints to accurately describe the process of scattering through the target with the electromagnetic matrix elements as an input parameters. For this proposal, we have assumed the measured value of $\langle 0_1^+||E2||2_1^+\rangle = 15.9(9)$ $e$fm^2 [16, 25] to estimate the γ-ray intensities. Simulations were performed assuming spectroscopic quadrupole moments guided by the MCSM calculations [2]. The assumption that $Q_s = 0$ $e$fm^2 yields 70 γ-ray counts per day in the $2_1^+ \rightarrow 0_1^+$ transition, coincident with a projectiles or recoil scattered in the safe angular range. We expect a 20% intensity enhancement for $Q_s = 27$ $e$fm^2 [2] and a reduction in intensity by a similar factor for a negative spectroscopic quadrupole moment. In order to achieve sensitivity to $Q_s(2_1^+)$, the data must be segmented in angular ranges and the statistics in each must be significant. It has been calculated that five days of beam time and five angular ranges provide the minimum conditions to achieve a precision of < 10 $e$fm^2 in $Q_s(2_1^+)$, as can be seen in the analysis of simulated data in Figure 3. The beam time request is summarised in Table 1. The data will be normalised to the excitation of the ^{206}Pb target, chosen since it has the appropriate kinematics and excitation cross sections as well as producing a de-excitation γ-ray spectrum that is as clean as possible. Simultaneously, an independent measurement of $B(E2; 2_1^+ \rightarrow 0_1^+)$ will be made to a precision of $\approx 10\%$, an improvement on, and verification of, the previous measurements. The techniques used are described in Ref. [26].

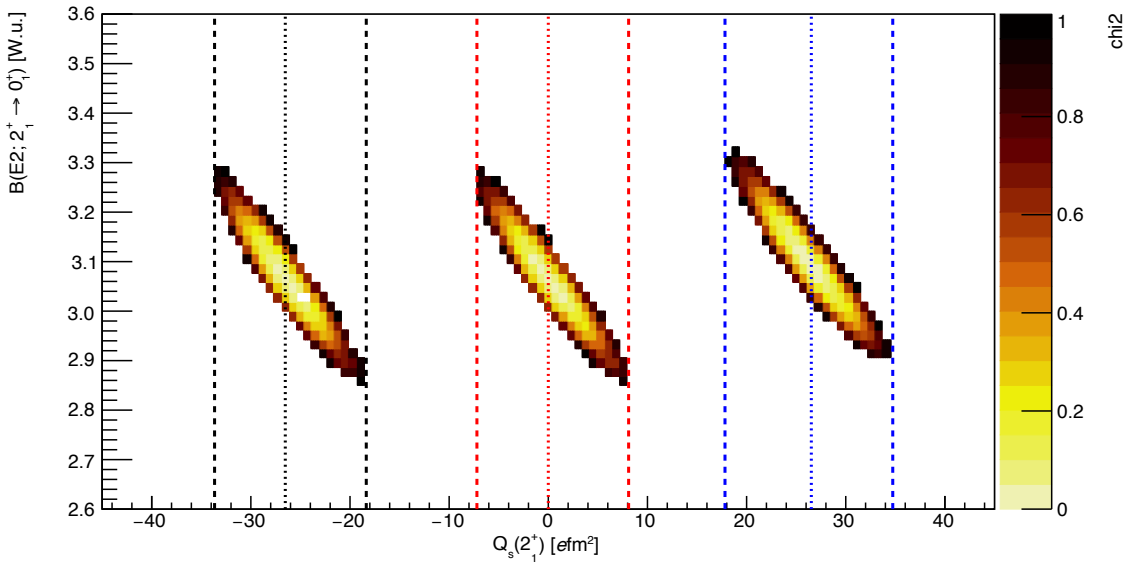

Figure 3: A simulated two-dimensional χ^2 surface plot, for the transitional and diagonal matrix elements (fit parameters) of the 2_1^+ state in ^{68}Ni. It is cut at $\chi^2_{\rm min}+1$ representing the 1σ contour. For this simulation, five centre-of-mass-angular slices were assumed corresponding to four projectile and one target solutions in the laboratory frame. The uncertainties on the γ-ray intensities were assumed to be statistical plus a 3% systematic uncertainty from the determination of the relative efficiency for detecting γ rays from the projectile and target.

^{66}Ni and ^{70}Ni – The kinematics of each of the three cases presented are very similar and it is proposed to follow the same analysis procedure as described for the ^{68}Ni part of the experiment. In the case of ^{66}Ni, there is an increase in the production yield (1.0×10^8 ions/μC [27]) and excitation cross sections over ^{68}Ni, giving an expected number of $2_1^+\rightarrow0_1^+$ γ rays/day of 10000, assuming a maximum rate of 2×10^6 ions/s at Miniball. At the same time, we expect to populate the 0_2^+ state, leading to a measurement of the $B(E2;0_2^+\rightarrow2_1^+)$ value, with $\approx$ 500 counts/day expected in the $0_2^+\rightarrow2_1^+$ γ-ray transition at a beam energy of 4.0 MeV/u. We therefore request 4 shifts to complete the aims of the ^{66}Ni experiment.
For ^{70}Ni, the production yield is lower (1×10^5 ions/μC [28]) and determining $Q_s(2_1^+)$ to sufficient precision will be challenging, even though the lower energy of the 2_1^+ state leads to a larger cross section than the ^{68}Ni case. However, as can be observed in Figure 3, the $B(E2;2_1^+\rightarrow0_1^+)$ value is strongly correlated to $Q_s(2_1^+)$ meaning that a significant number of counts is still required after segmentation of data into angular ranges, in order to determine the $B(E2;2_1^+\rightarrow0_1^+)$ value. From experience of similar experiments [29–31], at least three angular ranges are required. Due to the isobaric contamination expected at $A=70$, we require that 50% of the beam time is run with the RILIS lasers off. This laser on/off mode has been used previously in Coulomb-excitation experiments where normalisation to target excitation is required [31] in order to subtract the observed excitation due to contaminants. As mentioned in Section 1, there are two conflicting results from lifetime measurements and intermediate energy Coulex that yield $B(E2;2_1^+\rightarrow0_1^+)$ values of 2.7 W.u. and 10 W.u., respectively. We expect to observe a total of 28 or 100 γ-ray counts per day in the $2_1^+\rightarrow0_1^+$ transition for the respective $B(E2)$ values. To allow for proper discrimination of these potential results, including the requirement to segment the data, we estimate that 12 shifts are required for the ^{70}Ni experiment, leading to an estimated uncertainty of $\approx$ 20% in $B(E2;2_1^+\rightarrow0_1^+)$. For a 0_2^+ state at 1.567 MeV, we would expect less than ten γ-ray counts in the $0_2^+\rightarrow2_1^+$ transition over the entire running period.

Table 1: Summary of the beam-time request. The primary yield is taken to be the intensity of the 1^+ ions from the primary target, injected to the REX linac. We assume a proton current of 2 μA, a post-acceleration efficiency of 5% and a maximum rate of 2×10^6 ions/s is at Miniball. In addition, we expect a rate of 170 γ-ray counts/shift in the $0_2^+ \rightarrow 2_1^+$ transition of ^{66}Ni at 0.546 MeV. For the depopulation of the 0_2^+ state in ^{68}Ni, the method of detecting 511 keV γ rays following the $E0$ pair-production decay [1] yields six 511 keV γ-ray counts/shift.

	$T_{1/2}$	Primary yield	Beam Energy	$E_\gamma(2_1^+ \rightarrow 0_1^+)$	$I_\gamma(2_1^+ \rightarrow 0_1^+)$	$I_\gamma(^{206}\mathrm{Pb})$	Shifts
^{66}Ni	54.6 h	1×10^8 ions/μC	4.0 MeV/u	1.425 MeV	3400/shift	5000/shift	4
^{68}Ni	29 s	1×10^6 ions/μC	4.0 MeV/u	2.033 MeV	24/shift	250/shift	15
^{70}Ni	6 s	1×10^5 ions/μC	3.5 MeV/u	1.260 MeV	9 or 32/shift	15/shift	12

Competing and complementary experiments – Intermediate-energy Coulomb-excitation experiments have been performed at GANIL for ^{66}Ni and ^{68}Ni [25]. These data have intrinsic uncertainties (aside from the large statistical uncertainties) due to the potential for unobserved feeding from higher-lying 2^+ states and must be verified at safe energies or via direct lifetime measurements. In the case of ^{68}Ni, the $B(E2; 2_1^+ \rightarrow 0_1^+)$ was remeasured at REX-ISOLDE [16], where a total of eleven γ-ray counts were observed. Utilising HIE-ISOLDE energies to approach closer to the Coulomb barrier, the sensitivity to the spectroscopic quadrupole moment, $Q_s(2_1^+)$, will be improved. In ^{66}Ni, this experiment represents the first verification of the intermediate-energy result [25] and the first measurement of $Q_s(2_1^+)$, giving the shape of the charge distribution. Furthermore, populating the non-yrast states via multi-step Coulex will yield electromagnetic properties of the proposed shape-coexisting states, not accessible with other methods.
In the heavier masses, intermediate-energy Coulomb excitation at NSCL [7] has been used to determine $B(E2; 2_1^+ \rightarrow 0_1^+)$ in ^{74}Ni. This is the most neutron-rich nickel isotope studied in this way to date. Recent direct lifetime measurements performed at NSCL with the TRIPLEX plunger and GRETINA [10] have determined both $B(E2; 2_1^+ \rightarrow 0_1^+)$ and $B(E2; 4_1^+ \rightarrow 2_1^+)$ in ^{72}Ni with an uncertainty of 14% and 18%, respectively. However, data taken for ^{70}Ni at the same time has not yielded a reliable result and only an estimate for $B(E2; 2_1^+ \rightarrow 0_1^+)$ is available that is a factor of four smaller than the intermediate energy Coulex result [18]. Coulomb excitation at safe energies, proposed here, would provide an unambiguous determination of this value with $\approx 20\%$ uncertainty. In the lighter, stable isotopes, precision Coulomb-excitation measurements at HRIBF (ORNL) [32] have recently improved the knowledge of the $B(E2; 2_1^+ \rightarrow 0_1^+)$ systematics in the nickel isotopic chain.

Summary of requested shifts: In total we are requesting **33 shifts** in this proposal including 31 shifts to achieve the physics aims plus two shifts for setup of the RILIS, the beam and mass changes. This is in addition to the 9 shifts already granted for the $1n$-transfer part of the proposal.

References

[1] L. P. Gaffney, K. Kolos, F. Flavigny, and M. Zielinska, CERN-INTC **042**, P-398 (2013).
[2] Y. Tsunoda, T. Otsuka, N. Shimizu, M. Honma, and Y. Utsuno, Phys. Rev. C **89**, 031301 (2014).
[3] Y. Utsuno et al., Proc. Conf. Adv. Radioact. Isot. Sci. **6**, 010007 (2015).

[4] F. Recchia et al., Phys. Rev. C **88**, 041302 (2013).
[5] S. Suchyta et al., Phys. Rev. C **89**, 021301 (2014).
[6] J. Diriken et al., Phys. Lett. B **736**, 533 (2014).
[7] T. Marchi et al., Phys. Rev. Lett. **113**, 182501 (2014).
[8] C. J. Prokop et al., Phys. Rev. C **92**, 061302 (2015).
[9] J. Diriken et al., Phys. Rev. C **91**, 054321 (2015).
[10] K. Kolos et al., Phys. Rev. Lett. **116**, 122502 (2016).
[11] F. Nowacki, A. Poves, E. Caurier, and B. Bounthong, arXiv:1605.05103 (2016).
[12] S. M. Lenzi, F. Nowacki, A. Poves, and K. Sieja, Phys. Rev. C **82**, 054301 (2010).
[13] R. Orlandi et al., Phys. Lett. B **740**, 298 (2015).
[14] X. F. Yang et al., Phys. Rev. Lett. **116**, 182502 (2016).
[15] A. Gottardo et al., Phys. Rev. Lett. **116**, 182501 (2016).
[16] N. Bree et al., Phys. Rev. C **78**, 047301 (2008).
[17] C. Sotty et al., CERN-INTC **051**, P-402 (2013).
[18] O. Perru et al., Phys. Rev. Lett. **96**, 232501 (2006).
[19] D. Miller et al., Bull. Am. Phys. Soc. **55**, DC.00001 (2010).
[20] G. Breit, R. Gluckstern, and J. Russell, Phys. Rev. **103**, 727 (1956).
[21] N. Warr et al., Eur. Phys. J. A **49**, 40 (2013).
[22] V. Bildstein et al., Eur. Phys. J. A **48**, 85 (2012).
[23] T. Czosnyka, D. Cline, and C. Y. Wu, Bull. Am. Phys. Soc. **28**, 745 (1983).
[24] D. Cline et al., *Gosia User Manual for Simulation and Analysis of Coulomb Excitation Experiments*, `http://www.pas.rochester.edu/~cline/Gosia/Gosia_Manual_20120510.pdf`, Rochester, NY, US, 2012.
[25] O. Sorlin et al., Phys. Rev. Lett. **88**, 092501 (2002).
[26] M. Zielińska et al., Eur. Phys. J. A **52**, 99 (2016).
[27] ISOLDE Yield Database.
[28] T. Stora, (private communications), 2013.
[29] M. Albers et al., Nucl. Phys. A **899**, 1 (2013).
[30] L. P. Gaffney et al., Phys. Rev. C **91**, 064313 (2015).
[31] N. Kesteloot et al., Phys. Rev. C **92**, 054301 (2015).
[32] J. M. Allmond et al., Phys. Rev. C **90**, 034309 (2014).

Appendix

DESCRIPTION OF THE PROPOSED EXPERIMENT

The experimental setup comprises: MINIBALL + T-REX

Part of the	Availability	Design and manufacturing
MINIBALL + T-REX	☒ Existing	☒ To be used without any modification

HAZARDS GENERATED BY THE EXPERIMENT: Hazards named in the document relevant for the fixed MINIBALL + T-REX installation.

Additional hazards:

Hazards	^{66,68,70}Ni Coulex	
Thermodynamic and fluidic		
Pressure	[pressure][Bar], [volume][l]	
Vacuum		
Temperature	[temperature] [K]	
Heat transfer		
Thermal properties of materials		
Cryogenic fluid	LN_2, [pressure][Bar], [volume][l]	
Electrical and electromagnetic		
Electricity	[voltage] [V], [current][A]	
Static electricity		
Magnetic field	[magnetic field] [T]	
Batteries	☐	
Capacitors	☐	
Ionizing radiation		
Target material [material]		
Beam particle type (e, p, ions, etc)		
Beam intensity		
Beam energy		
Cooling liquids	[liquid]	
Gases	[gas]	
Calibration sources:	☒	
• Open source	☐	
• Sealed source	☒	
• Isotope	^{152}Eu(4205RP)/^{133}Ba(4206RP)	
• Activity	23.64 kBq/22.32 kBq	
Use of activated material:		
• Description	☐	
• Dose rate on contact and in 10 cm distance	[dose][mSV]	
• Isotope		
• Activity		
Non-ionizing radiation		
Laser	RILIS	

UV light		
Microwaves (300MHz-30 GHz)		
Radiofrequency (1-300 MHz)		
Chemical		
Toxic	[chemical agent], [quantity]	
Harmful	[chem. agent], [quant.]	
CMR (carcinogens, mutagens and substances toxic to reproduction)	[chem. agent], [quant.]	
Corrosive	[chem. agent], [quant.]	
Irritant	[chem. agent], [quant.]	
Flammable	[chem. agent], [quant.]	
Oxidizing	[chem. agent], [quant.]	
Explosiveness	[chem. agent], [quant.]	
Asphyxiant	[chem. agent], [quant.]	
Dangerous for the environment	[chem. agent], [quant.]	
Mechanical		
Physical impact or mechanical energy (moving parts)	[location]	
Mechanical properties (Sharp, rough, slippery)	[location]	
Vibration	[location]	
Vehicles and Means of Transport	[location]	
Noise		
Frequency	[frequency],[Hz]	
Intensity		
Physical		
Confined spaces	[location]	
High workplaces	[location]	
Access to high workplaces	[location]	
Obstructions in passageways	[location]	
Manual handling	[location]	
Poor ergonomics	[location]	

Hazard identification:

Average electrical power requirements (excluding fixed ISOLDE-installation mentioned above): [make a rough estimate of the total power consumption of the additional equipment used in the experiment]: ... kW